

Face-sheet/core debonds in composite sandwich structures – fusion of full-field imaging data and FE simulations

H. L. Emily Leung*, Riccardo Cappello, Janice M. Dulieu-Barton, and Ole T. Thomsen

*emily.leung@bristol.ac.uk

Bristol Composites Institute, School of Civil, Aerospace, and Mechanical Engineering, University of Bristol, UK



Motivation

Composite Sandwich Structures

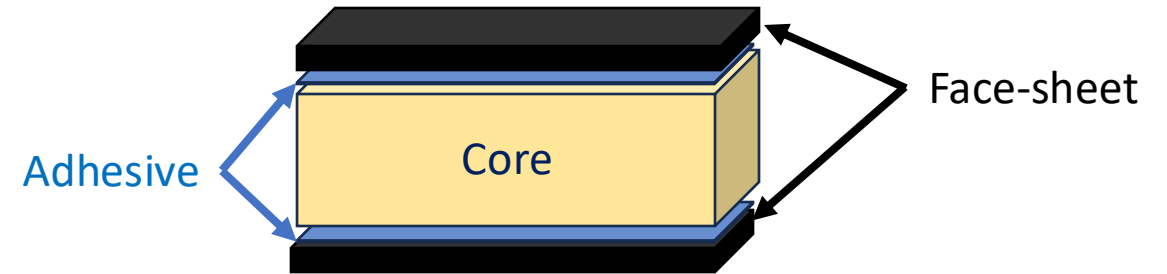
- High bending stiffness and strength to weight ratio



Motivation

Composite Sandwich Structures

- High bending stiffness and strength to weight ratio



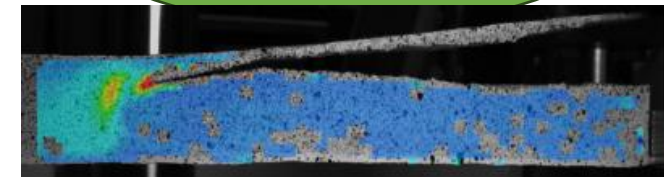
Background

Damage in sandwich structures

- Reduced stiffness and strength



View of damaged area



Martakos et al [1]

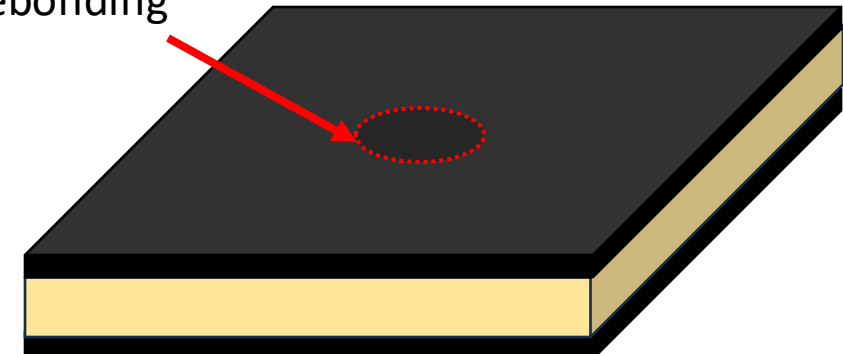
Previous studies

- Crack tip
- Subsequent damage propagation at the face-sheet/core interface can be identified

Large structures

- Difficult to access and view hidden damaged area

Face-sheet/core debonding

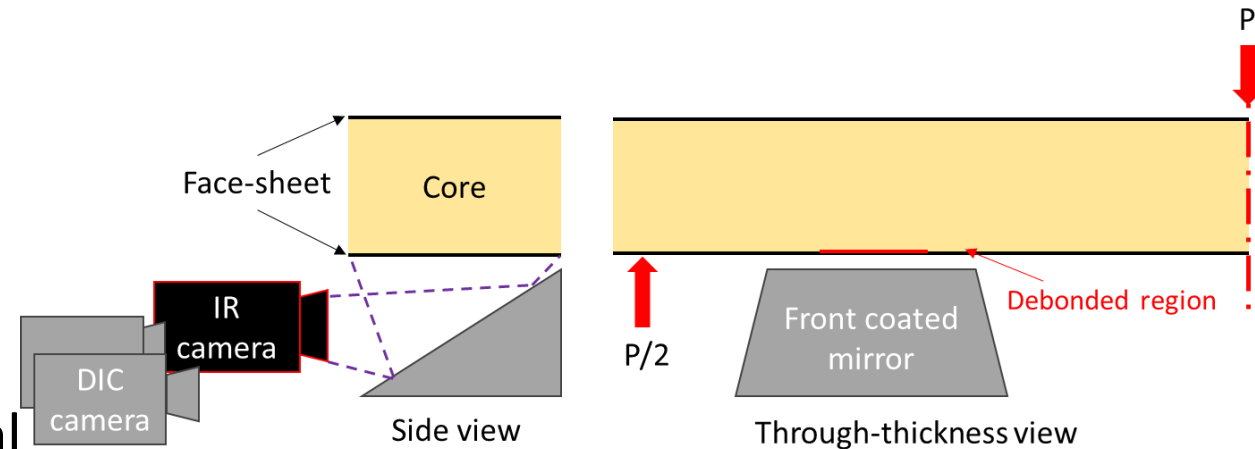


[1] Martakos G, Andreasen J, Berggreen C, Thomsen O. Experimental investigation of interfacial crack arrest in sandwich beams subjected to fatigue loading using a novel crack arresting device. Journal of Sandwich Structures & Materials. 2019;21(2):401-421. doi:10.1177/1099636217695057

Aims/Objectives

Identify face-sheet/core interface debonding through the thin face-sheets of sandwich beams

- Use mirror-assisted imaging methodology to view inaccessible regions and extend the field of view of cameras
- Detect debond at the interface
 - Digital image correlation(DIC)
 - Thermoelastic stress analysis (TSA)
- Finite Element (FE) model
 - Validation of FE models by experimental data



Thermoelastic stress analysis (TSA)

TSA utilizes the thermoelastic effect to correlate the temperature variations and the stresses in a structure subjected to elastic cyclic loading

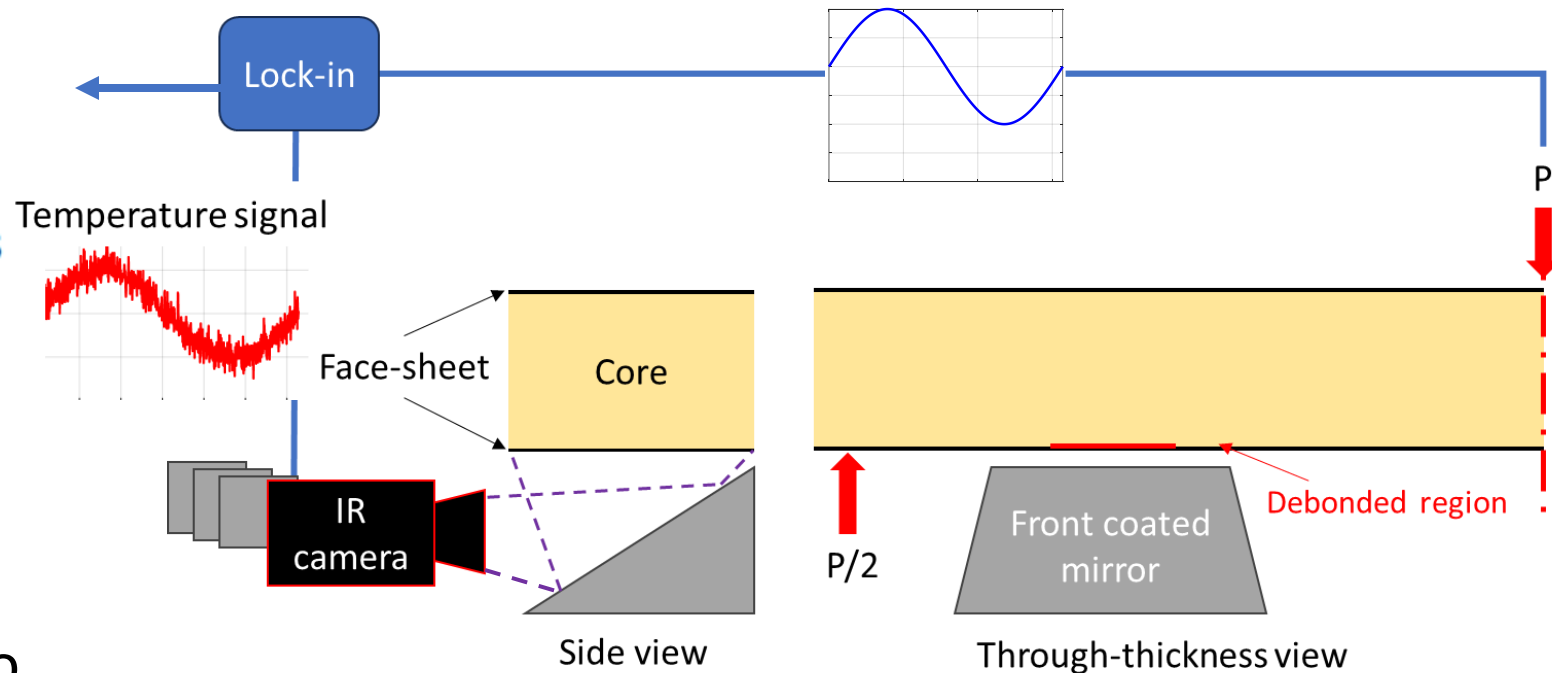
Thermoelastic response, ΔT

$$\dot{T} = \frac{T_0}{\rho C_\varepsilon} \frac{d\sigma_{ij}}{dT} \varepsilon_{ij} - \frac{\dot{Q}}{\rho C_\varepsilon} \quad \text{for } i, j = 1, 2, 3$$

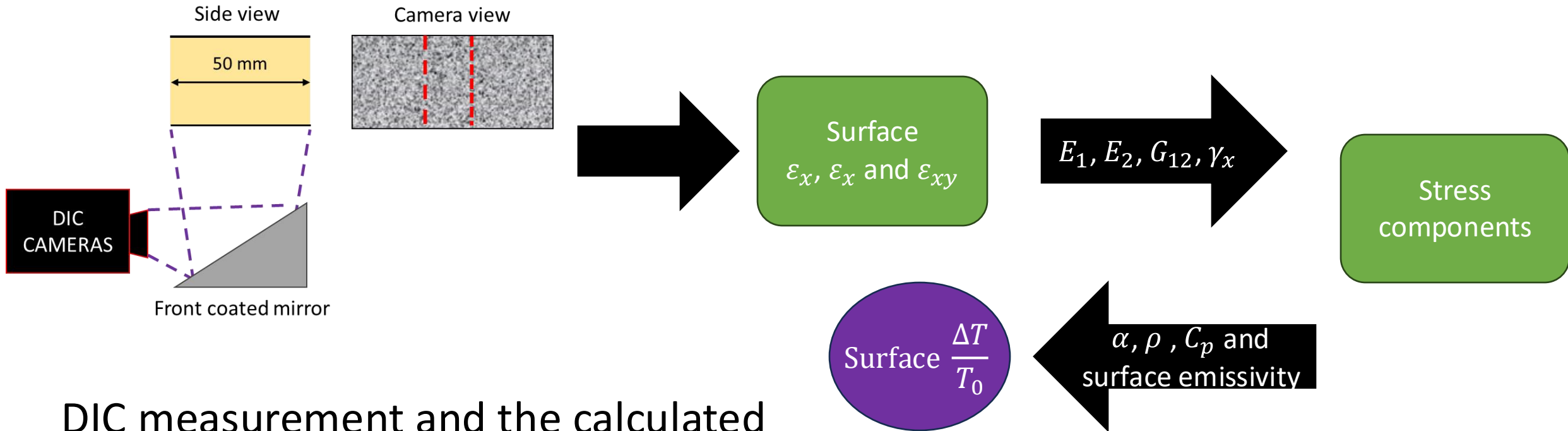
Heat transfer term

$$\frac{\Delta T}{T_0} = - \frac{(\alpha_1 \Delta \sigma_1 + \alpha_2 \Delta \sigma_2)}{\rho C_p}$$

A high loading frequency is used to ensure adiabatic conditions

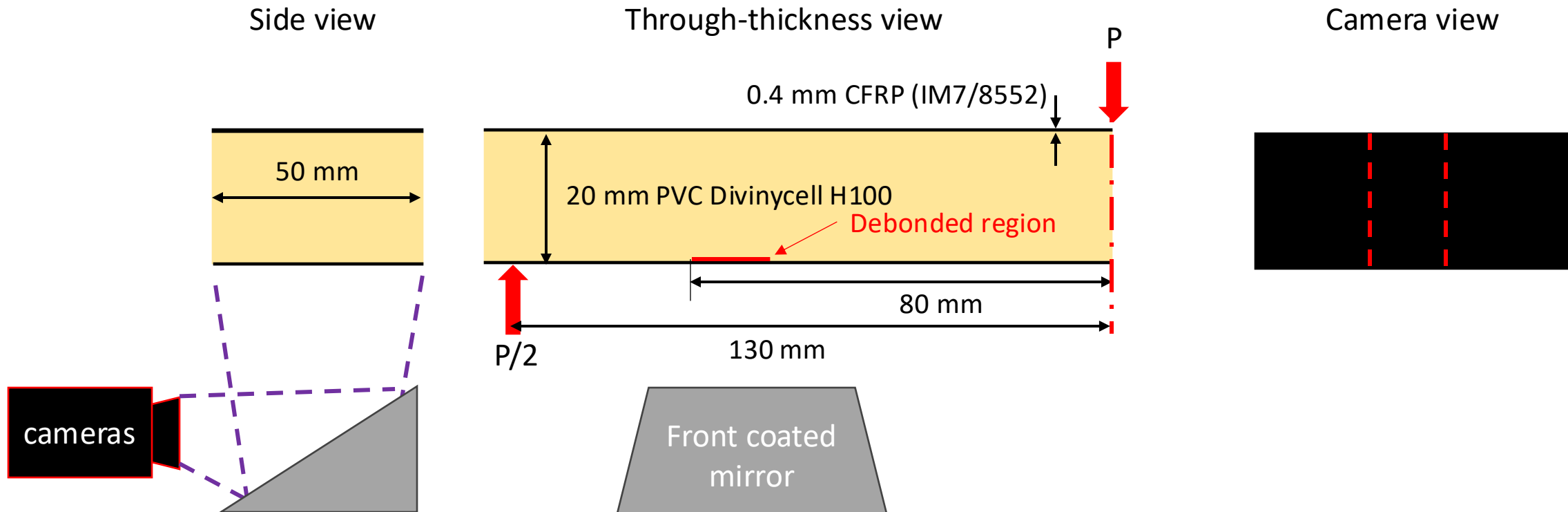


Combining TSA and DIC

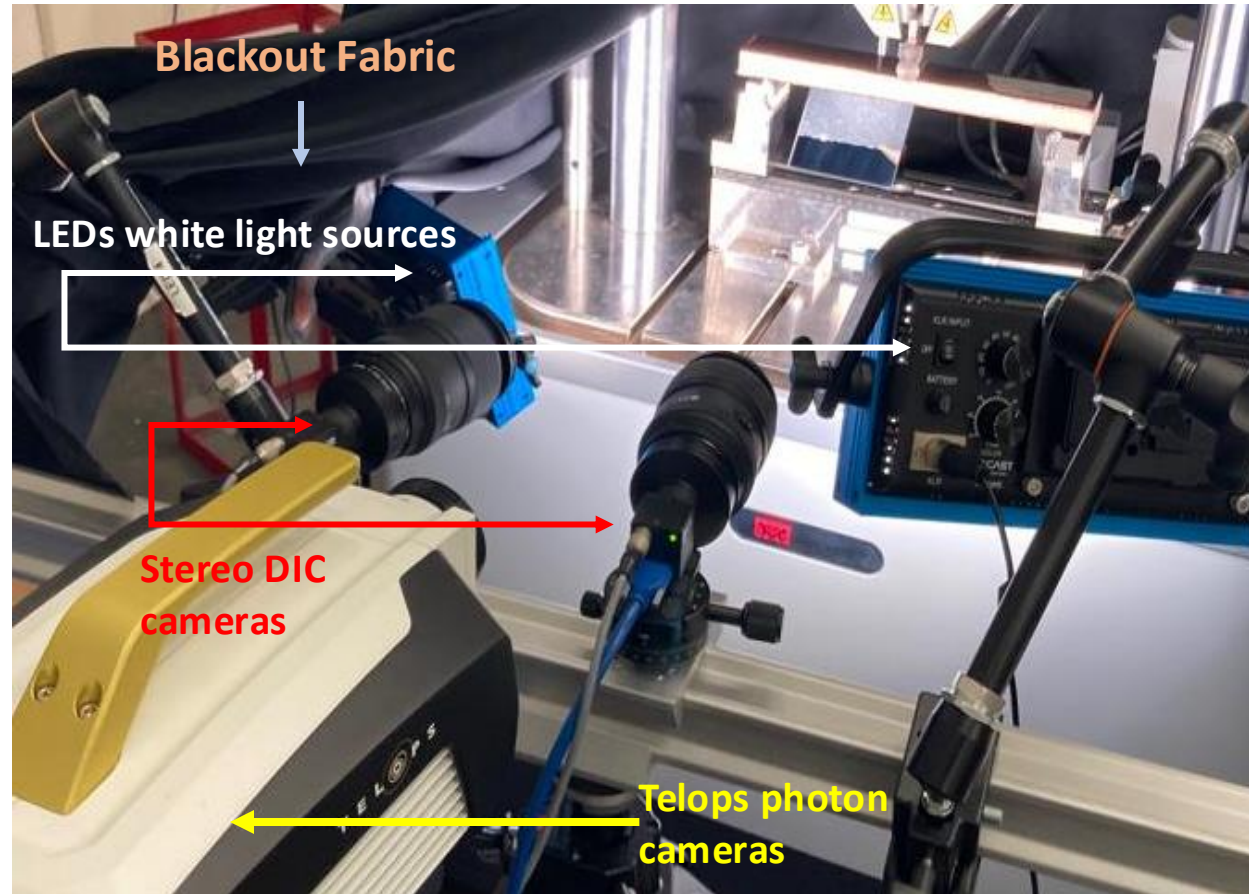


DIC measurement and the calculated surface $\frac{\Delta T}{T_0}$ are independent of the heat diffusion effect

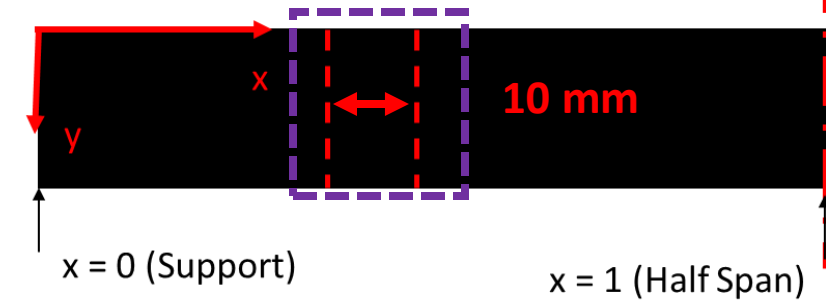
Specimen and loading configuration



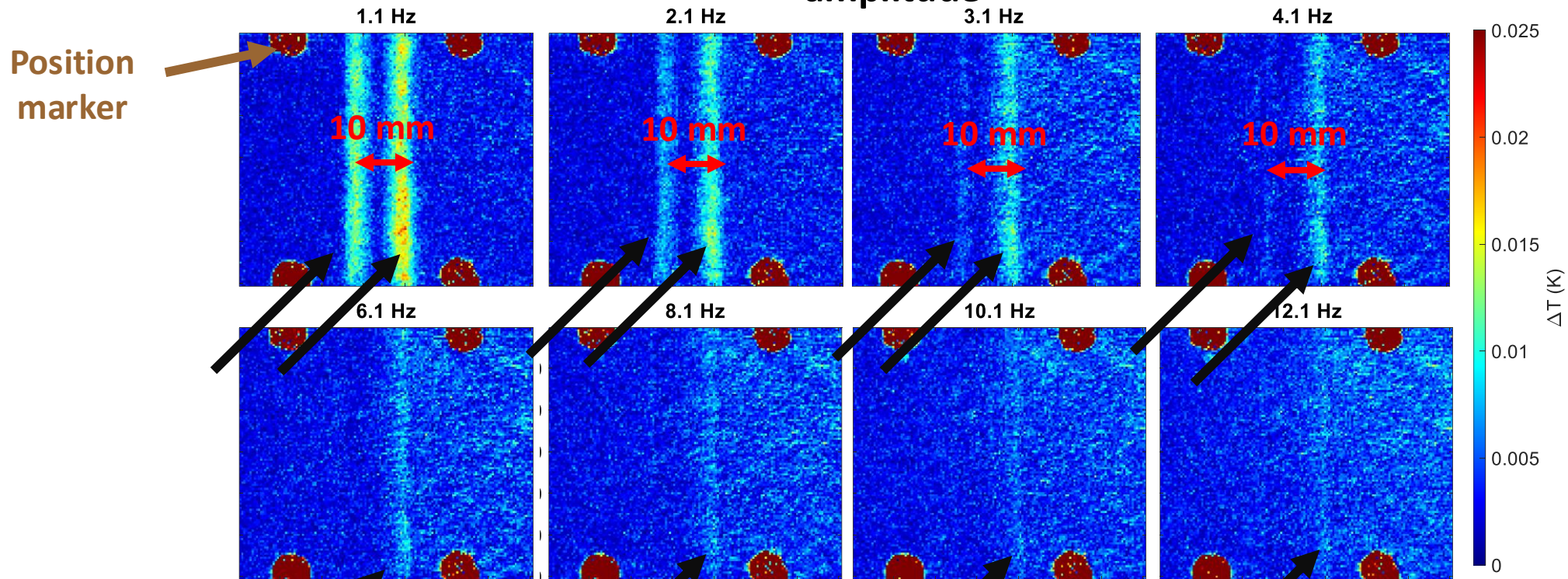
Experimental set-up



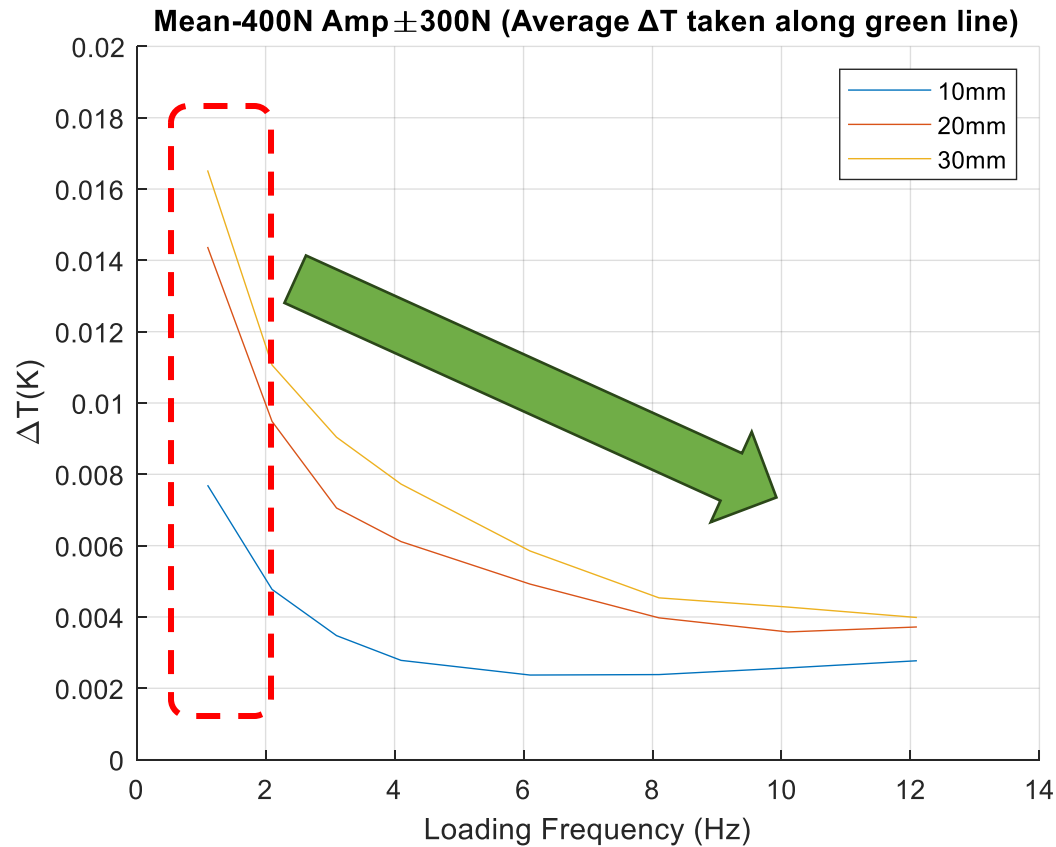
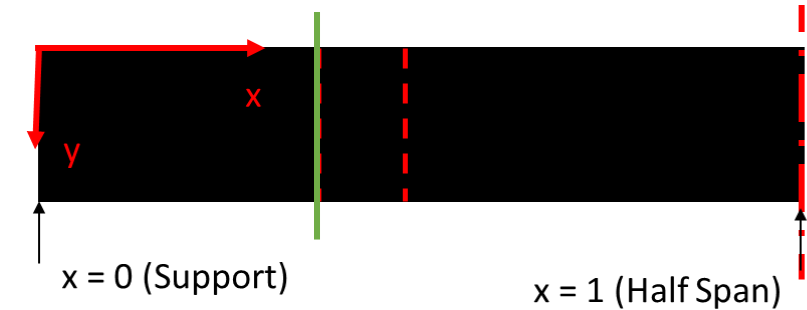
Thermoelastic response



10mm debonded specimen loaded at -550N mean load with ± 450 N amplitude



Effect of debond size on ΔT



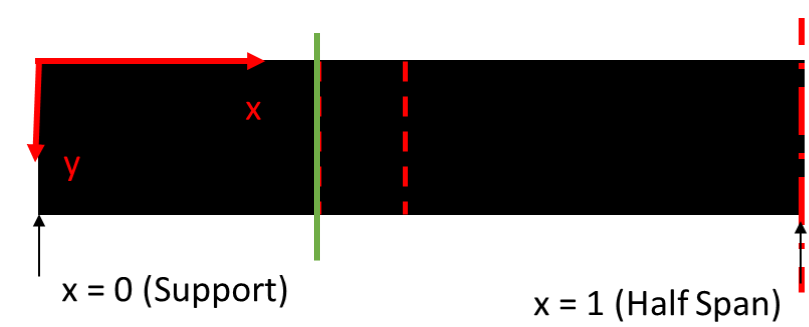
Trends are similar regardless of debond size

- High thermoelastic response at low loading frequencies
- Decreases with increased loading frequencies
- Trend plateaus above 8Hz

Specimens with larger debond sizes

- Higher thermoelastic response
- Unable to transfer longitudinal stress in the debonded region
- ΔT at 30 mm > 20 mm > 10 mm

Effect of loading amplitude

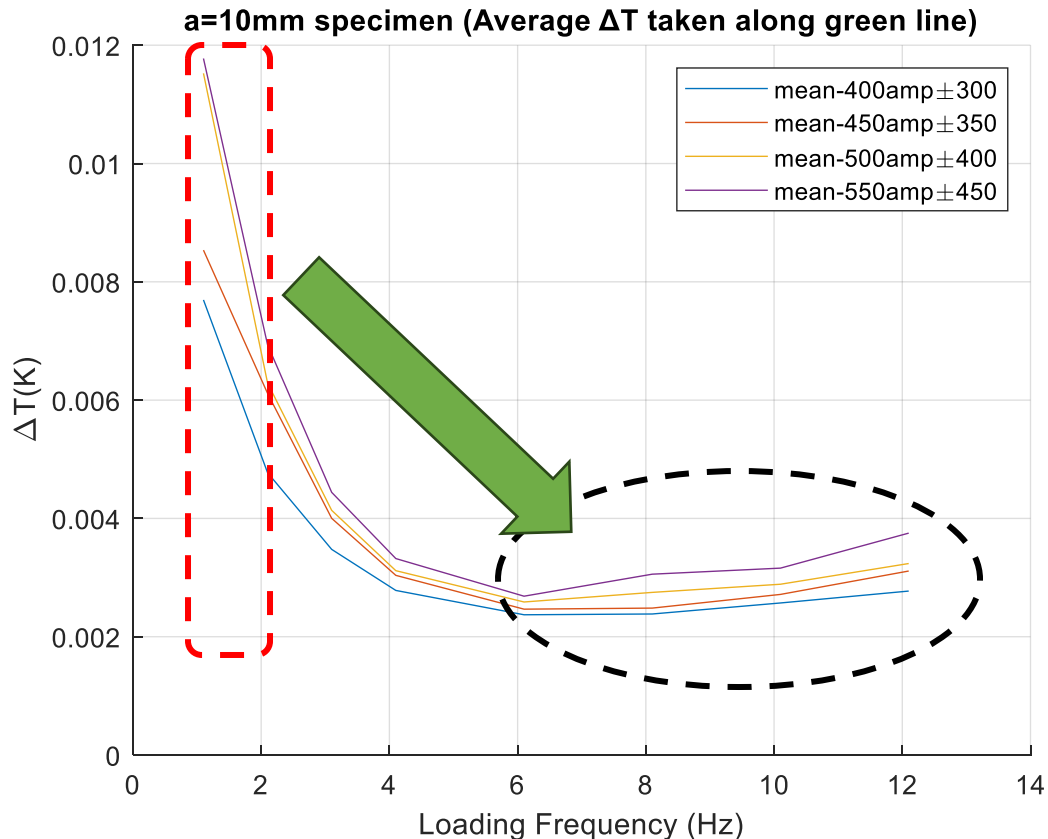


Specimens loaded at higher amplitudes give higher thermoelastic responses

Trends are similar regardless of loading amplitude

- Increased thermoelastic response after 6 Hz

To observe the damaged region at the interface through the face-sheets, heat conduction from the sub-surface is required



Investigation of face-sheet/core interface

Thermoelastic Stress Analysis (TSA)

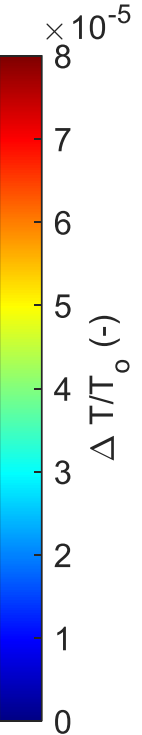
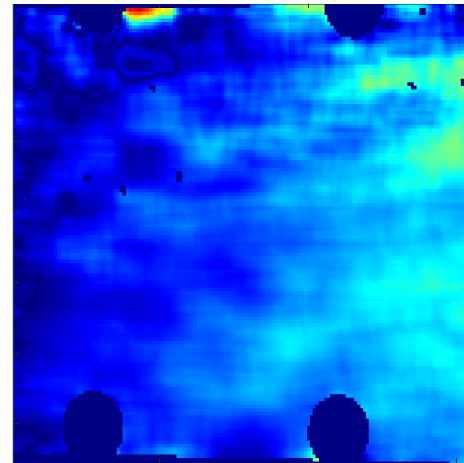
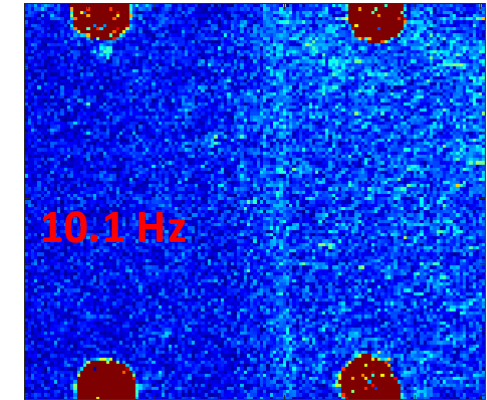
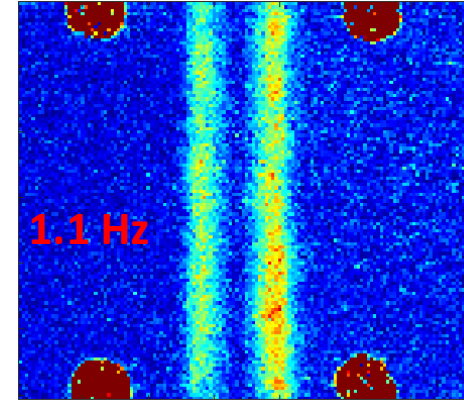
Obtains the thermoelastic response at the damaged region at different frequencies

$$\frac{\Delta T}{T_0} = \frac{(\alpha_1 \Delta \sigma_1 + \alpha_2 \Delta \sigma_2)}{\rho C_p}$$

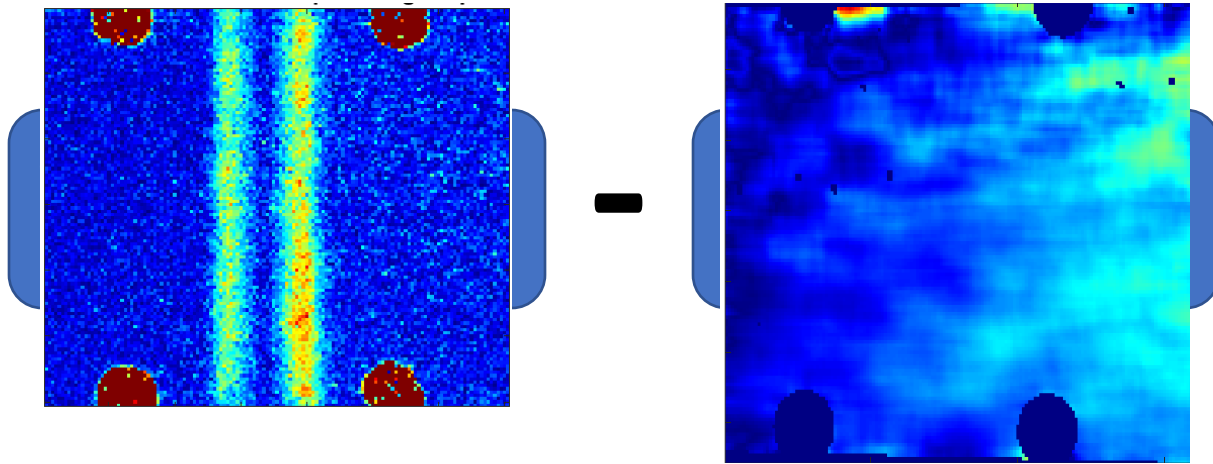
Digital Image Correlation (DIC)

Obtains **surface ply** thermoelastic response

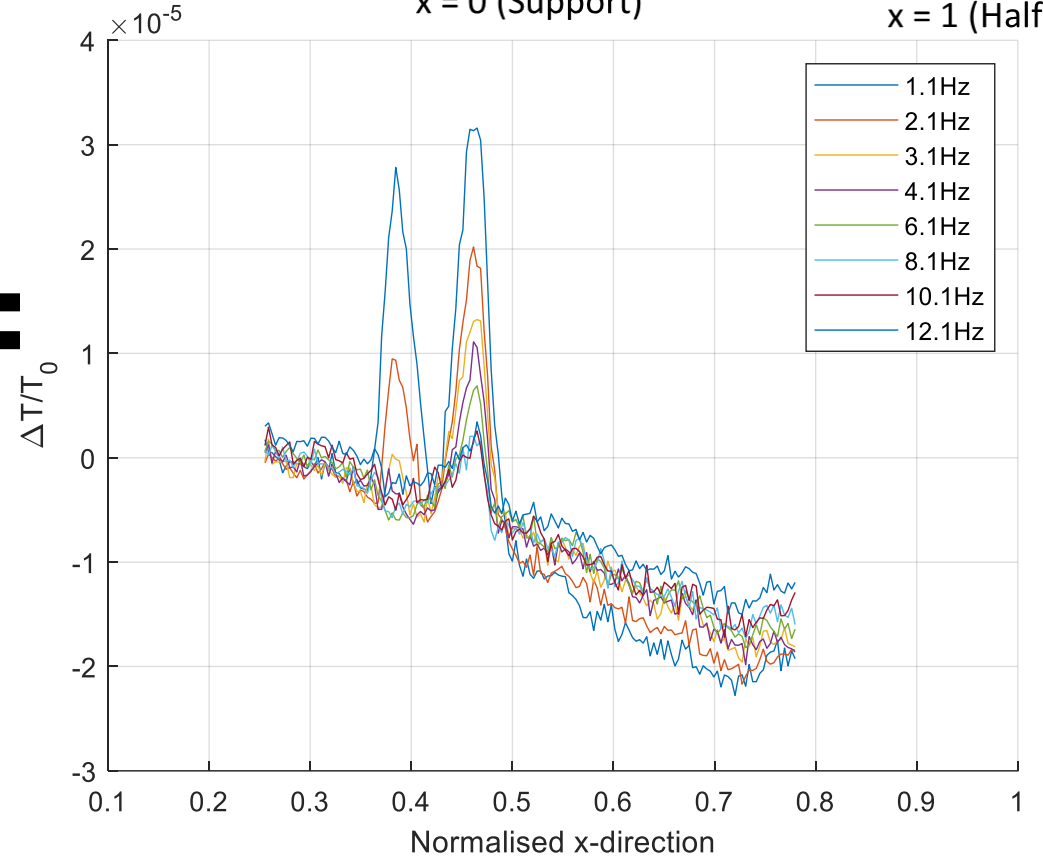
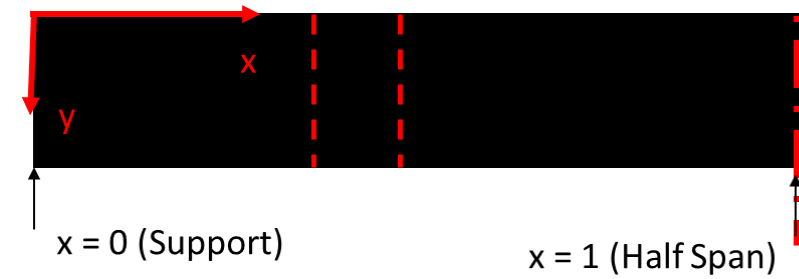
$$\frac{\Delta T_{surfaceply}}{T_0} = -\frac{e}{\rho C_p} [\alpha_1 \quad \alpha_2 \quad 0] \begin{bmatrix} \frac{E_1}{1-\nu_{12}\nu_{21}} & \frac{\nu_{21}E_1}{1-\nu_{12}\nu_{21}} & 0 \\ \frac{\nu_{21}E_1}{1-\nu_{12}\nu_{21}} & \frac{E_2}{1-\nu_{12}\nu_{21}} & 0 \\ 0 & 0 & G_{12} \end{bmatrix} [T_e] \begin{bmatrix} \Delta \epsilon_x \\ \Delta \epsilon_y \\ \Delta \epsilon_{xy} \end{bmatrix}$$



Full-Field Data Fusion



Does this represent thermoelastic response at the interface ?



Modelling details

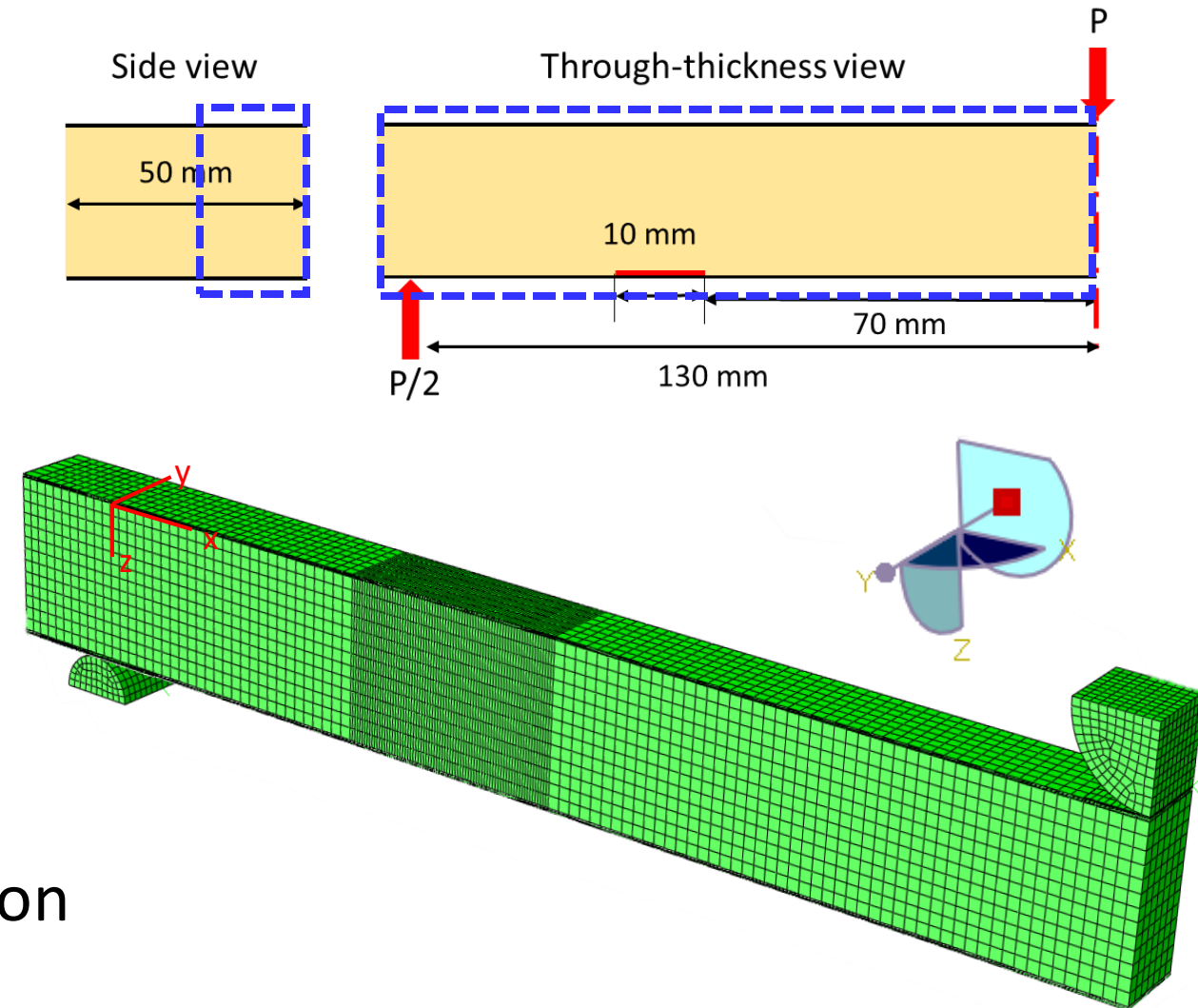
Geometric non-linear model

Element type

- C3D8T-8-node trilinear coupled temperature-displacement element (face-sheet and core)

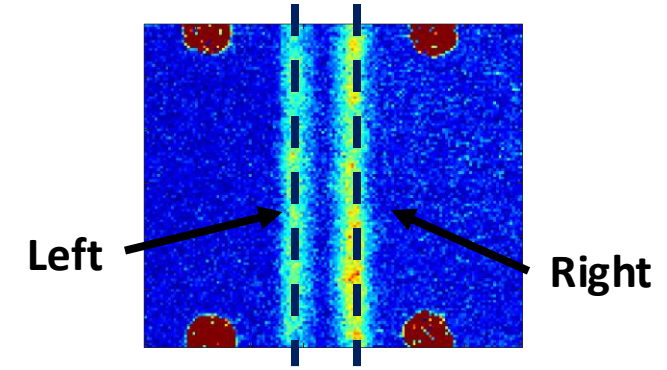
Fortran user subroutine [2] is used to generate synthetic TSA data

As an addition to the model, heat transfer is allowed at the debond region by using thermal contact.



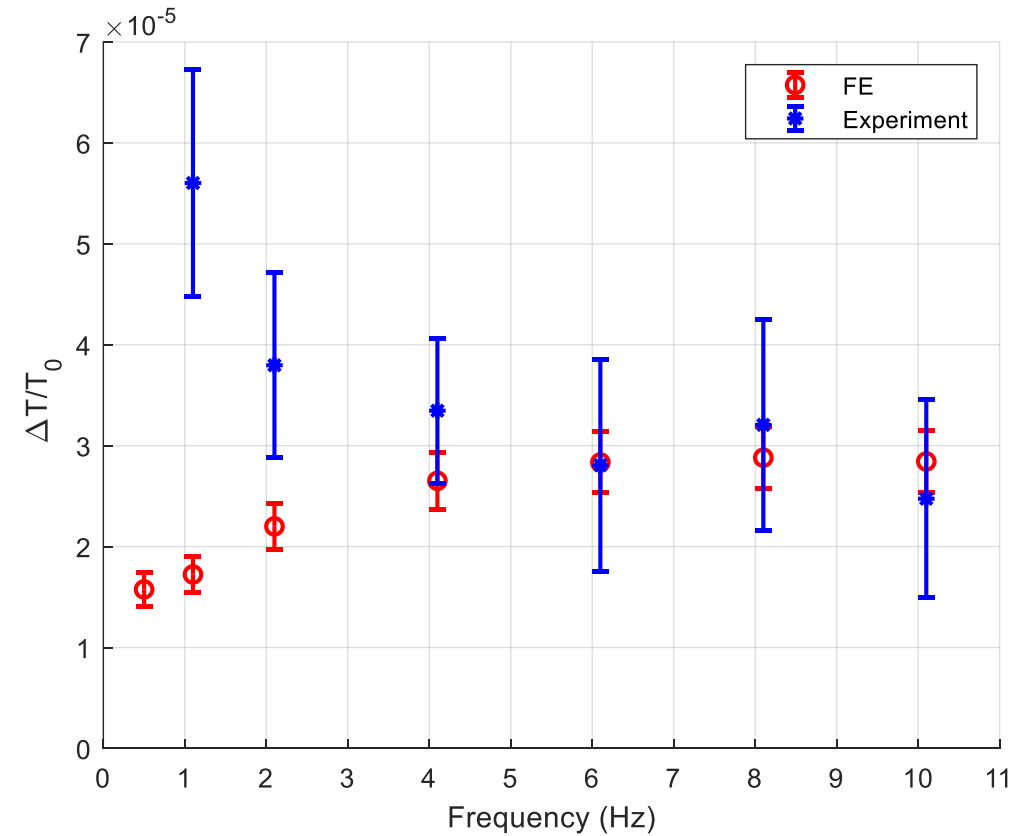
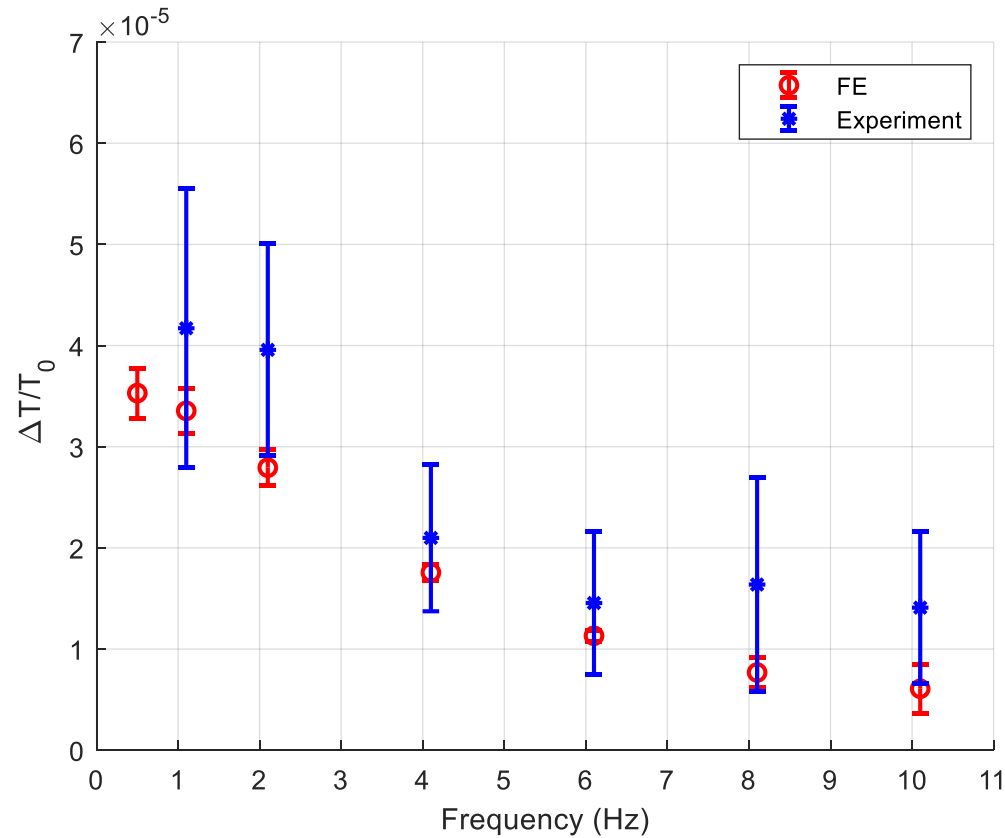
[2] Cappello, R., Pitarresi, G., Catalanotti, G.: Thermoelastic Stress Analysis for composite laminates: A numerical investigation. Compos Sci Technol. 241, 110103 (2023). <https://doi.org/10.1016/J.COMPSCITECH.2023.110103>

FE and Experimental data - $\Delta T/T_0$

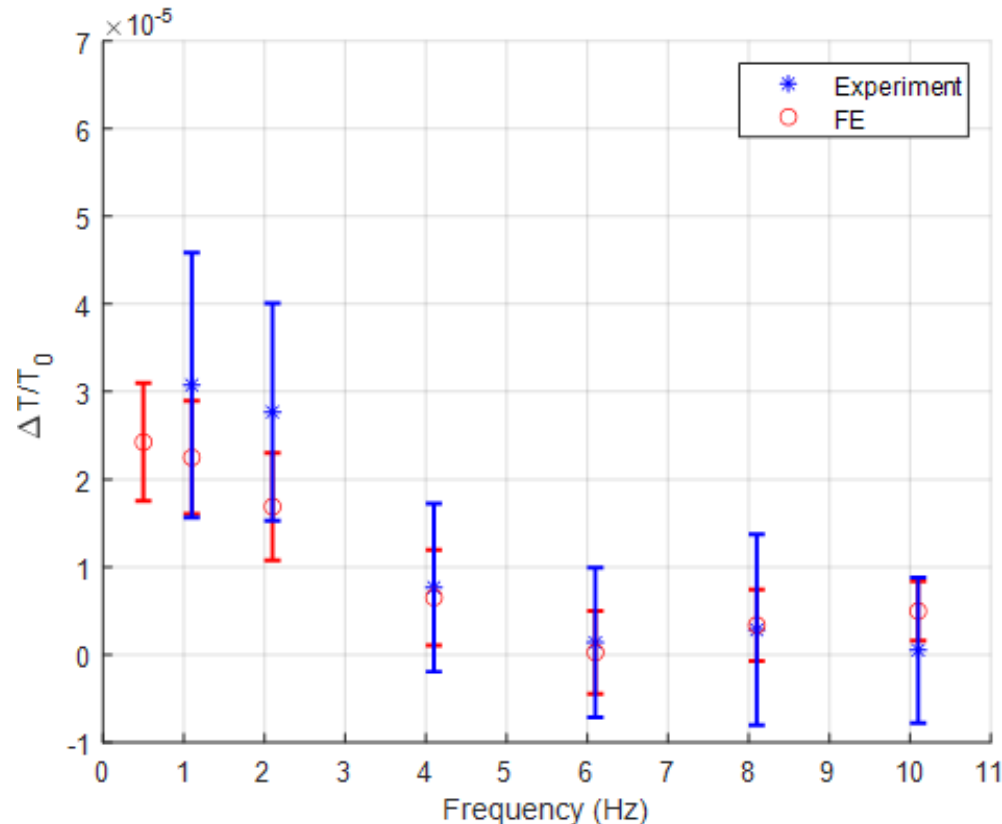


Left

Right



FE and Experimental fused data - 'Interface' $\Delta T/T_0$ at the left debond edge



Fused Experimental data

- TSA from IR – surface thermoelastic response from DIC

FE

- Surface thermoelastic response (1-11Hz)-
1000Hz surface thermoelastic response

Similar trend with the FE thermoelastic response

A representative 'interface' thermoelastic response is crucial

- Understand the heat transfer at the interface

Summary and Future work

Interface debonded regions were observed through the face-sheets using thermoelastic stress analysis, when cyclically loaded at low frequency

General agreement between the experimental and FE results was observed, discrepancies possibly explained by:

- Material properties
- Potential crack growth in the core on the right debonded edges

Agreement between the fused data and FE results

Future investigation the thermal behavior between the face-sheet and core under non-adiabatic conditions

- Investigate heat transfer effects and the source of thermoelastic response at the interface
- Relate ΔT to the damage severity at the interface